International Conferences on Recent Advances in Geotechnical Earthquake Engineering and Soil Dynamics

1991 - Second International Conference on Recent Advances in Geotechnical Earthquake Engineering & Soil Dynamics

12 Mar 1991, 2:30 pm - 3:30 pm

Pseudo- Three-Dimensional Analysis of Cyclic Deformation of Ground Subject to Seismic Liquefaction

Ikuo Towhata
Syracuse University, NY

M. D. Shafiqui Islam
Syracuse University, NY

Proceedings: Second International Conference on Recent Advances in Geotechnical Earthquake Engineering and Soil Dynamics, March 11-15, 1991, St. Louis, Missouri, Paper No. 8.10

Pseudo-Three-Dimensional Analysis of Cyclic Deformation of Ground Subject to Seismic Liquefaction

Ikuo Towhata
Associate Professor of Civil Engineering

M.D. Shafiqul Islam
Graduate Student, Syracuse University

SYNOPSIS: A Numerical tool was developed to evaluate the effects of differential movement which occurs at the ground surface during earthquakes. A special emphasis is placed on liquefaction of subsoils. A complicated three-dimensional analysis was avoided by using a pseudo-three-dimensional method of finite element analysis which runs on an element mesh of the ground surface topography as seen from the sky. The present analysis takes into account the nonlinear stress-strain behavior of soils, the ground softening due to pore pressure development, and the irregularity in the topography. The proposed method was applied to several cases in which buried pipelines were damaged by seismic liquefaction. The calculated results showed that the differential movement of the ground in cyclic manners is not significant. Thus, it seems that those pipeline failures were induced not by the cyclic ground movement but by the monotonic or permanent displacement which accumulated to several meters.

INTRODUCTION

The present research is concerned with the mechanism of failures which occur to buried pipeline networks in the course of seismic liquefaction. Hamada et al. (1986) studied those failures which took place in Noshiro City in 1983, detecting a permanent ground displacement of several meters in the lateral directions. Since the permanent displacement of this magnitude resulted in a significant ground deformation, it was speculated that a substantial axial force and bending moment, greater than the strength, were induced in the pipeline body, leading to its breakage.

It should be noted that there is another possible cause of pipeline failures. The acceleration history recorded at a liquefied site (e.g. basement of a Kawagishi-Cho apartment building in Niigata) revealed that the predominant period of the motion became much longer than the normal value due to soil liquefaction, accompanied by an increased acceleration amplitude. It seems, therefore, that the dynamic component of the ground-surface displacement is much greater after the onset of subsoil liquefaction when the ground is softer than before liquefaction. The ground displacement of a large amplitude easily leads to a large differential displacement or a ground deformation along the route of buried pipelines.

A numerical analysis to evaluate the differential cyclic motion at the ground surface was thus desired in order to compare the significance of the static permanent displacement with the cyclic differential movement.

A buried pipeline network normally has bends and branches. An irregular topography of the ground surface and a local variation of soil conditions are not rare. The horizontal component of the ground motion occurs in both EW and NS direction. These issues require a three-dimensional version of analysis which is of a nonlinear dynamic type. It is well known, however, that an analysis of this kind is very difficult because of a lack of a suitable deformation model for soils, a complicated evaluation of soil parameters, and a lengthy computation time.

A boundary element method is able to make some contribution to develop a three-dimensional analysis of the ground. However, most of the methods so far reported run on a linearly elastic ground. Furthermore, many of them assume a harmonic excitation of the ground under which soil properties do not vary with time. This state of arts obviously conflicts with the reality in which soils have a nonlinear stress-strain relationship and the development of excess pore water pressure makes soil softer with time.

The first author of this text carried out a pseudo-three-dimensional analysis on the permanent displacement of a liquefied ground wherein the surface unsaturated layer was modeled by a two-dimensional plane-stress finite element of linear elasticity, while the liquefied sublayer was replaced by a frictionless inclined floor (Towhata, 1986). This method was developed further to be a dynamic version (Towhata, 1987). Note that a special emphasis is placed on the effects of subsoil liquefaction, which is the most important difference of the present study from a similar method that was proposed by Tamura and Suzuki (1987) almost at the same time but independently.

FINITE ELEMENT MODEL OF PSEUDO-THREE-DIMENSIONAL CONFIGURATION

Fig.1 illustrates a schematic view of the proposed method. The unsaturated surface soil layer which does not liquefy is modeled by plane-stress finite elements, while the liquefiable subsoil situated between the ground water table and the unliquefiable "base" is modeled by a spring and a dashpot (Voigt model). Both the finite element at the surface and the Voigt model underneath are of viscoelastic characteristics. The nature of the Voigt model is exactly identical in both x and y directions, allowing for a multi-directional shaking of the base.

It is seen in Fig.1 that the thickness of the finite elements is not constant. This is because of the variable level of the ground water table and the irregular surface topography. Properties of the finite elements as well as the Voigt model will be discussed later on.

The baserock motion is of multi-directional nature, occurring in both x and y, or EW and NS, directions simultaneously. It is possible to consider, if necessary, the delay of wave incidence due to the limited rate of S-wave propagation in the base.

The side boundaries are temporarily free of stress, although some modification in future is desired to take into account the lateral infinity of the ground. Hence, the calculated response of the ground near the side boundary is subject to a certain amount of error. However, this error hardly propagates to the interior of the model due to the viscosity which is assigned to the finite elements as well as dashpots.

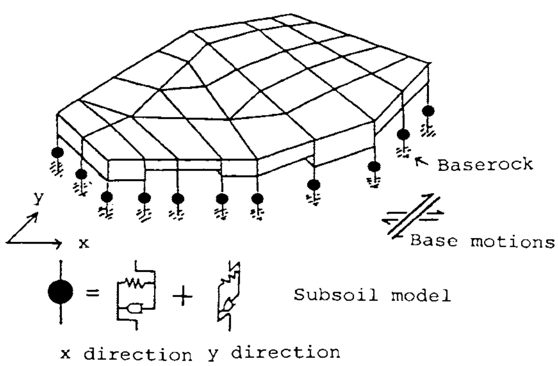

Fig.1 Schematic view of pseudo-3-D finite element model

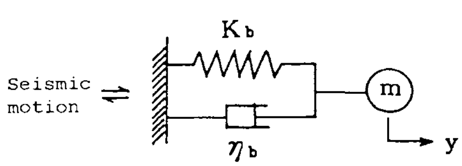

Fig.2 Single-degree-of-freedom model composed of lumped mass and Voigt model.

ELASTIC PROPERTIES OF FINITE ELEMENTS AND VOIG MODEL

The dynamic analysis on the model in Fig.1 i carried out in the time domain by integratin the equation of motion;

$$[M]\ddot{u}+[C_g]\dot{u}+[K_g]u=-[C_b](\dot{u}-\dot{u}_g)-[K_b](u-u_g) \qquad (1$$

where u is the absolute displacement of th nodal points at the ground surface, u_g is th displacement of the base, and dots indicate the time derivative. Those matrices [M], $[C_g]$ and $[K_g]$ are the mass, viscosity, and stiffnes matrices of the finite element model at th surface, whilst $[C_b]$ and $[K_b]$ stand for th viscosity and the stiffness of the Voigt mode at the bottom. Visco-linear-elasticity is thu assumed to both finite elements and Voig models. However, the values of viscous an elastic parameters mentioned above are variable, varying with time corresponding to th magnitude of strain and development of exces pore water pressure. The finite element mode employs a lumped-mass method. Hence, each nodal point is associated with a mass which is denoted by m in what follows.

Fig.2 illustrates a single-degree-of-freedom model thus constructed, in which K_b and η_b represents the spring stiffness and the dashpot viscosity, respectively. The natural circular frequency, ω_o, of the model is given by

$$\omega_o = \sqrt{K_{b,max}/m} \qquad (2)$$

in which $K_{b,max}$ is the value of K_b at very small shear distortion of the liquefiable subsoil. Since the mass, m, is known, $K_{b,max}$ can be evaluated in accordance with a given natural circular frequency, ω_o, of the ground at a particular nodal point. Note that $K_{b,max}$ indicates the ground stiffness at the beginning of a seismic event.

The Young modulus, E, and the Poisson ratio, υ, of the surface finite element can be evaluated empirically by using, e.g., standard penetration test data. They are then replaced by the bulk modulus, B, and the shear modulus, G_{max}, at a small strain amplitude;

$$B = \frac{E}{2(1-\upsilon)} \qquad G_{max} = \frac{E}{2(1+\upsilon)} \qquad (3)$$

The B parameter is maintained constant throughout the period of response analysis unless liquefaction in the subsoil triggers a boiling of sand which destroys the surface layer.

EFFECTS OF SHEAR STRAIN AND PORE WATER PRESSURE DEVELOPMENT ON ELASTIC PROPERTIES OF MODEL

The spring stiffness of the Voigt model, K_b, should be altered in accordance with the magnitude of the maximum shear strain, $\gamma_{b,max}$, as well as the developed excess pore water pressure, P, in the subsoil.

Fig.3 is indicative of the variation of spring stiffness with the intensity of shear strain. This figure is similar to the famous G vs. γ curve of soils (Seed and Idriss, 1970) because both K_b and G represent soil resistance against lateral displacement during shaking. The amplitude of shear strain, $\gamma_{b,max}$, in the subsoil is simply evaluated, although approximate, by

$$\gamma_{b,max} = U_{max}/H \tag{4}$$

$$U_{max} = Max\ (\ U_x{}^2 + U_y{}^2)\ \text{for}\ 0 \le t \le tm \tag{5}$$

where U_x and U_y are x- and y- components of the displacement at nodes relative to the base, while H is the thickness of the liquefiable layer that is represented by a Voigt model. The maximum displacement in Eq.5 is taken between the beginning of shaking and the current time, t_m. Eq.4 is most valid when a homogeneous level ground is at resonance of the fundamental mode, and is expected to be reasonable for the present simplified analysis, because a fundamental mode of resonance is still predominant under an irregular excitation as will be shown in Fig.5 later.

Fig.4 reveals the modification of K_b modulus with the excess pore pressure development which degrades the soil stiffness. The present analysis does not predict the time history of excess pore pressure development, P. The P/σ_{vo}' history, in which σ_{vo}' stands for the initial effective overburden pressure, is specified intuitively from a design view point, although some attention may be paid to an effective stress analysis in 1-D manner (Ishihara and Towhata, 1980) which is performed separately. When the current value of σ_v'/σ_{vo}', the reduction of effective stress, is determined at t_m, the current K_b is obtained by an idea that soil stiffness at small strain is proportional to a power (commonly 0.5) of σ_v'.

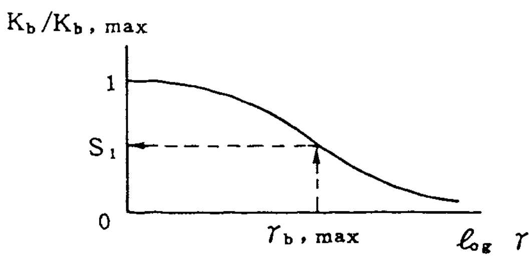

Fig.3 Variation of spring stiffness with shear strain.

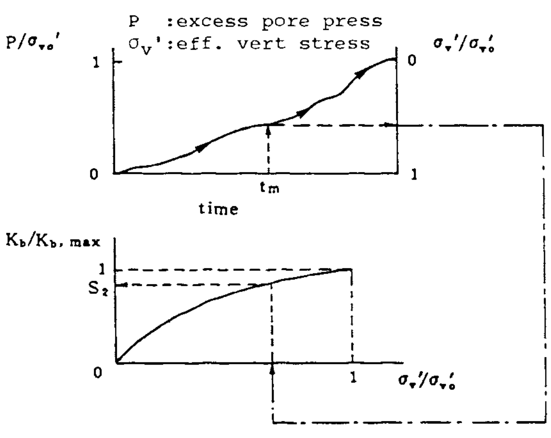

Fig.4 Degradation of spring stiffness with pore pressure development.

Thus, the current value of K_b modulus is obtained by

$$K_b = S_1\ S_2\ K_{b,max} \tag{6}$$

in which S_1 and S_2 are evaluated in Figures 3 and 4. The K_b value thus determined is employed for dynamic analysis from time t_m to $t_m + \Delta t_m$, and is then updated repeatedly.

The bulk and shear moduli, B and G, of the surface finite element are evaluated in a similar manner;

$$B = S_2\ (\text{initial B in Eq.3})$$
$$G = S_1\ S_2\ G_{max} \tag{7}$$

where S_1 stands for the effects of strain amplitude, $\gamma_{e,max}$, in the element, similar to Fig.3, whilst S_2 suddenly changes from 1 to 0 when a perfect liquefaction occurs in the subsoil to create a boiling and liquefy the surface layer. Using K_b, B, and G thus determined, the stiffness matrices $[K_g]$ and $[K_b]$ in Eq.1 are obtained.

EVALUATION OF VISCOUS MATRIX

The viscosity of the model is evaluated approximately by knowing a damping ratio. When a single-degree-of-freedom model in Fig.2 is subject to a harmonic motion, the deformation of the model (relative displacement of the mass) is expressed like

$$U = U_o\ (\omega)\ \cos \omega t \tag{8}$$

where the amplitude, U_o, is a function of frequency, ω. The energy dissipation per cycle, Δw, is given by

$$\Delta w = \int \eta_b \frac{dU}{dt}\ dU = \pi \eta_b \omega U_o{}^2 \tag{9}$$

The number of cycles included in the duration time T_D of shaking is equal to equal to $\omega T_D/2\pi$. Hence, the total energy dissipation, Δw, which occurs at the frequency of ω is given by

$$\Delta W = \Delta w \frac{\omega T_D}{2\pi} = \frac{1}{2} \eta_b T_D (\omega U_o)^2$$

$$= \frac{1}{2} \eta_b T_D V_o^2 \qquad (10)$$

in which V_o is the amplitude of relative velocity. Thus, the energy loss at a frequency ω is proportional to V_o^2 when the viscosity and the duration time are held constant.

Fig.5 indicates a spectrum of the total energy loss, V_o^2, when a single-degree-of-freedom model is excited by an irregular El Centro motion. Note that, when the stiffness of the model is varied over a natural period (T) ranging from 0.08 to 0.9 sec., the predominant energy loss occurs unexceptionally at the natural period, T. The energy loss due to the resonant component out of an irregular motion is the most influential. Thus, it is resolved that the viscosity of the Voigt model, η_b, is determined without a significant error in energy loss so that the model may attain the desired damping ratio, h_b, at the natural period or the current natural frequency, ω_o.

$$h_b = \frac{\text{Energy dissipation}}{4\pi\ (\text{Elastic energy})} = \frac{\eta_b \omega_o}{2K_b} \qquad (11)$$

$$\omega_o = \sqrt{K_b / m} \qquad (12)$$

The damping ratio is obtained from Fig.6 for which the maximum strain is calculated by Eq.4.

The element's viscosity matrix $[C_e]$ is obtained by

$$[C_e] = \frac{2h_e}{\omega} [K_e] \qquad (13)$$

in which the elementary damping ratio is determined by the element's shear strain that is maximum so far (similar to Fig.6) while ω is the average of the natural frequency at nodal points associating the particular element;

$$\omega = \omega_e = (\text{Average of } \omega_o \text{ at associating nodes}) \qquad (14)$$

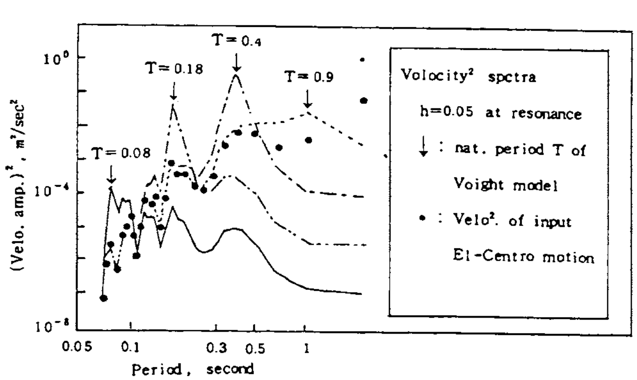

Fig.5 Relationship between energy loss and period of motion.

The determination of parameters so far describ ed is summarized in Fig.7. It should b emphasized that all the material properties ar updated repeatedly at such an appropriate tim interval as one second of shaking in accordanc with the pore pressure rise and the generate strain which is maximum up to the current time

CASE STUDIES

The method of analysis described above wa compiled into a FORTRAN computer code name "SAAM-D" in which "SAAM" means "THREE" in Thai. It was then applied to sites in the Noshir City where pipeline failures occurred an Hamada et al. (1986) detected a permanent ground strain of over one percent. The base motion employed here is the one which was recorded at the Akita Harbor during the concerned earthquake in 1983 and was converted to the base motion. For simplicity no delay was assumed in the wave incidence.

Analyzed areas were divided into liquefied and unliquefied domains by using such airphoto informations as cracks and sand boils (Hamada, et al. 1986). The liquefied domain in the analysis has a 100 % development of excess pore pressure at 12 seconds after the initiation of shaking, while the unliquefied area is associated with 33% pore pressure increment ($P/\sigma_{vo}' = 0.33$). Note that the spring stiffness was kept greater than 1% of its initial value, $K_{b,max}$, even after the complete liquefaction. This is because multi-directional simple shear tests on sand (Ishihara and Yamazaki, 1980) revealed that 100% pore pressure rise or zero effective stress is attained only at moments when shear stress in both x and y directions are equal to null accidentally at the same time, which rarely happens in reality where x and y motions of earthquakes occur almost independently.

The thickness of the subsoil is 10 m in the following analyses. Boiling and a breakage of the surface layers is not considered in the present calculation.

No.1 Site in Noshiro

The finite element model of this site is shown in Fig.8. Although the location of the buried pipeline is illustrated, the analysis does not take it into account. One of the breakage of

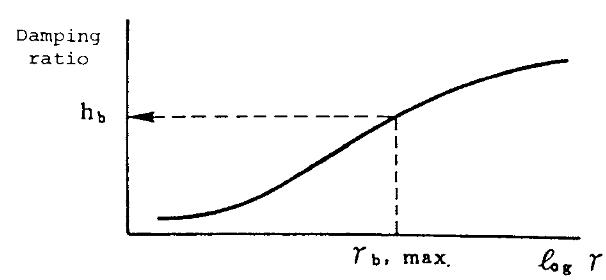

Fig.6 Relationship between damping ratio and strain amplitude.

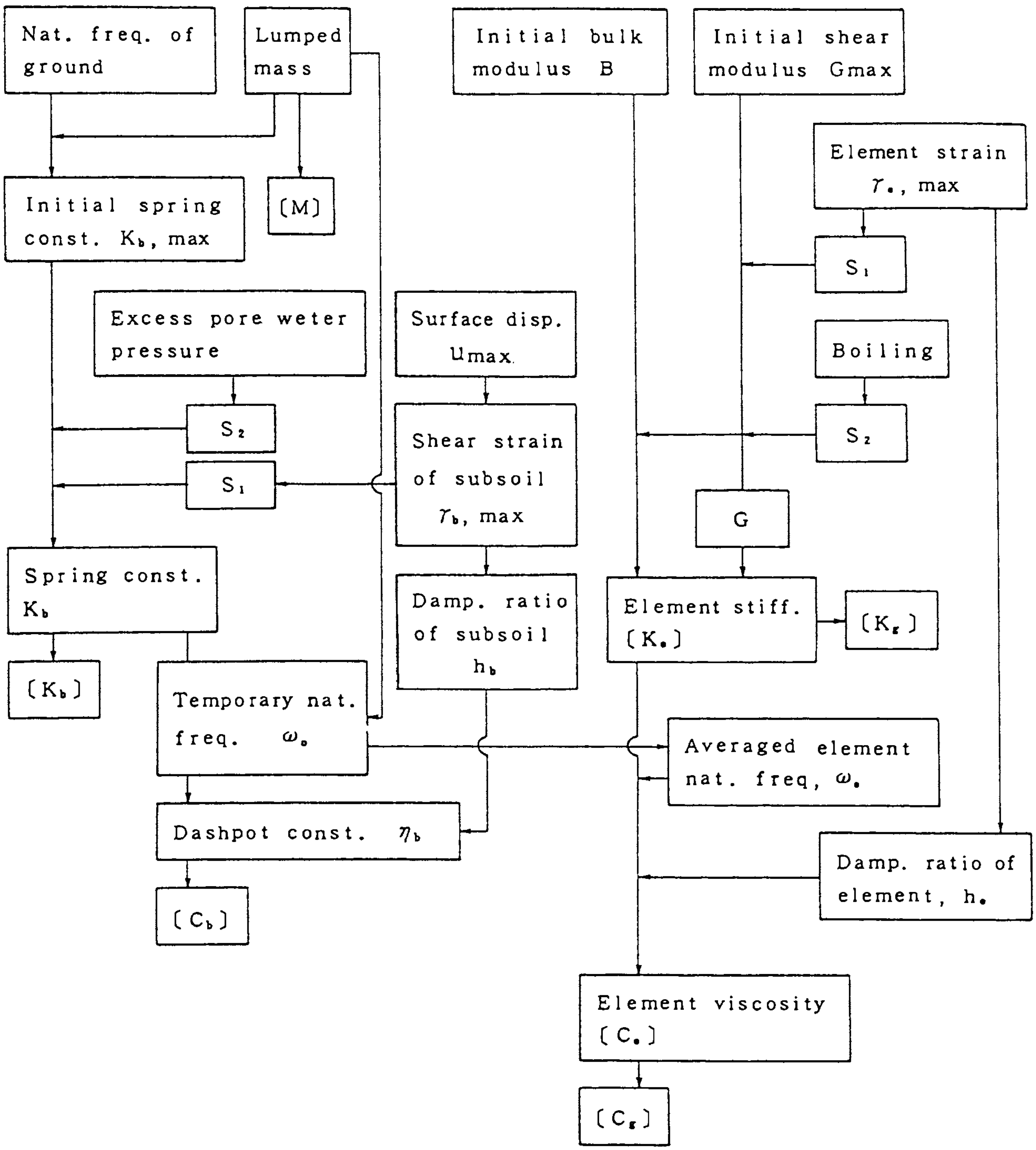

Fig.7 Flow chart for updating material properties and matrices.

pipe was detected at No.1 point in the figure. The soil liquefaction is supposed to have occurred in the shaded domain.

Fig.9 indicates the time history of calculated displacement difference derived between nodes no. 34 and 56. The maximum displacement is not more than 1cm over the distance of around 70 m. Deformation in unliquefied domain is as small as this. Hence, it seems difficult to relate this result to the pipeline breakage.

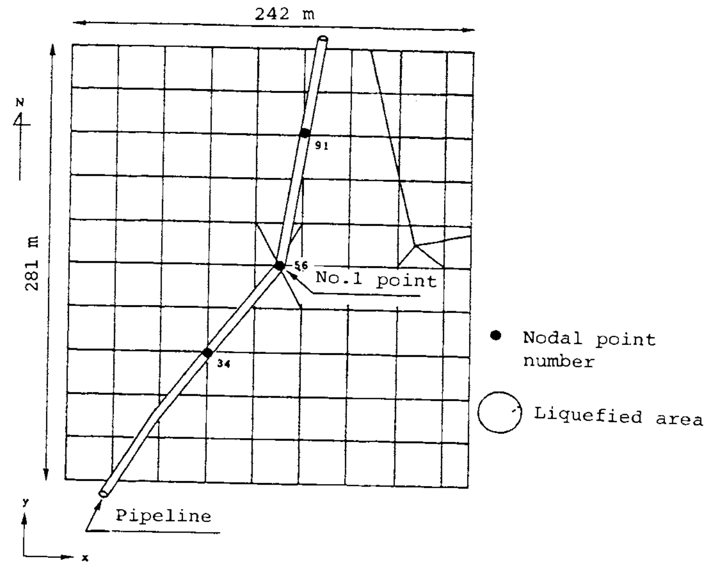

Fig.8 FE model of Noshiro No.1 site.

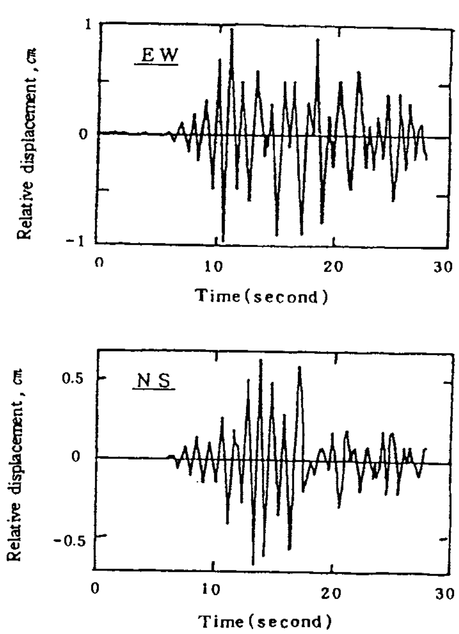

Fig.9 Time history of relative displacement between nodes 34 and 56 (Noshiro, No.1).

No.2 Site in Noshiro

The finite element model is illustrated i Fig.10. Pipeline failed at the node no. 61. comparison is made of acceleration time histor in Fig.11 between the node 24 in an unliquefie domain and the node 61 in a liquefied area The motion at node 61 is of longer period o motion than that at node 24. Particularly th elongated period after 100% liquefaction (1 seconds) is obvious.

Fig.12 shows the relative displacement histor between nodes 24 and 48 together with the on between nodes 60 and 71. No significant dis placement was detected even between nodes 2 and 48 between which there is a boundary o liquefied and unliquefied domains.

The most remarkable relative displacement wa found when the shear and bulk moduli of th surface finite element were reduced to 1% o the initial value in the liquefied domain wher the surface layer is considered to be broken b boiling sand and water. The maximum relativ displacement between nodes 24 and 61 (Fig.13, is 15 cm over a distance of 80 m.

DISCUSSION

Case history studies did not show a cyclic ground deformation as large as 1% which the permanent ground deformation attained. Hence, it is currently concluded that those pipeline failures detected in the particular area were caused by the permanent ground displacement, while the cyclic component is much smaller than the permanent one.

It should be pointed out, however, that the present analysis neglected the delay of wave incidence at the base which is one of the

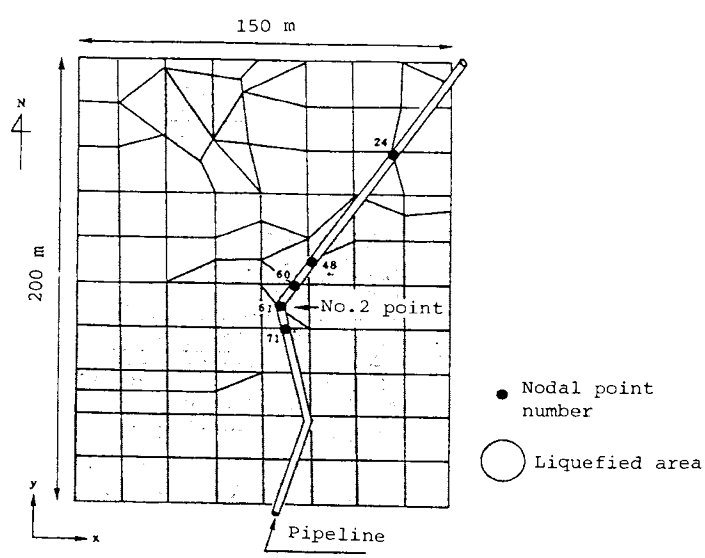

Fig.10 FE model of Noshiro No.2 site.

ources of relative displacement of the ground. oreover, the present simplified analysis can-ot take into account the surface wave propaga-ion. Further studies seem needed in these espects.

ONCLUSIONS

he cyclic component of the relative displace-ent or the deformation of ground was investi-ated by a newly developed pseudo-three-dimen-sional computer code. The following conclu-sions may be drawn from studies so far made.

1) It is possible to carry out a three-dimensional dynamic analysis in a simplified manner with effects of soil nonlinearity and pore pressure development taken into account.

2) The subsoil liquefaction affects the frequency of the surface motion.

3) The cyclic ground displacement seems less significant than the static permanent one in their effects on ground deformation. Thus, the latter is probably the main cause of the damages which occurred to pipelines in the studied area.

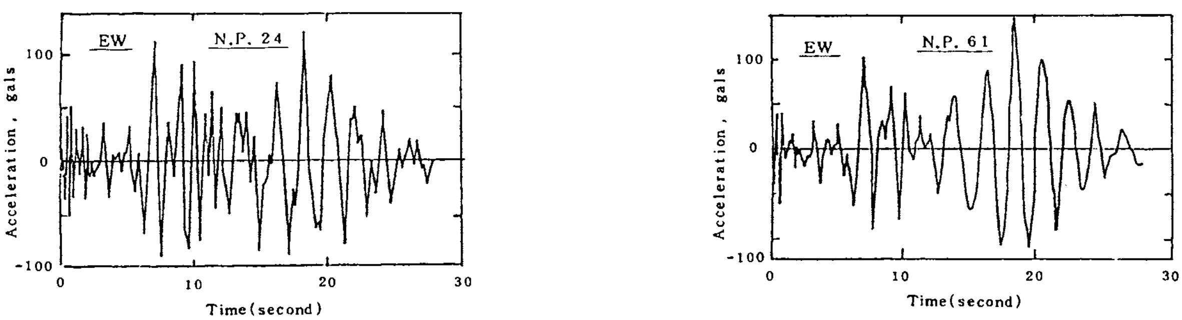

Fig.11 Time history of surface acceleration in liquefied and unliquefied domains (Noshiro No.2).

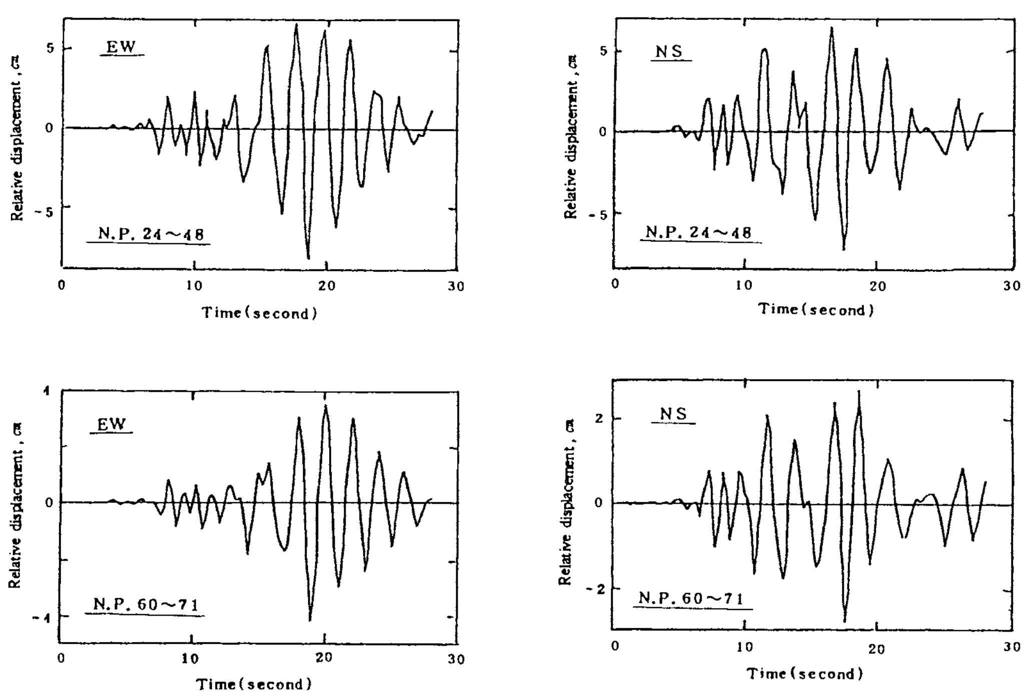

Fig.12 Time history of relative displacement of ground (Noshiro No.2).

ACKNOWLEDGMENT

The present study was conducted at the Asian Institute of Technology, Bangkok, under a financial assistance from the Association for Development of Earthquake Prediction (ADEP), Tokyo. All the supports given to the authors are deeply appreciated.

LIST OF REFERENCES

Hamada,M., S.Yasuda, R.Isoyama, and K.Emoto (1986) "Study on Liquefaction Induced Permanent Ground Displacements", ADEP, Tokyo.

Ishihara, K. and I.Towhata (1980) "Dynamic Response Analysis of Level Ground Based on the Effective Stress Method", Soil Mechanics - Transient Cyclic Loads, Ed. Pande and Zienkiewicz, John Wiley and Sons, 133-172.

Ishihara,K. and Yamazaki,F. (1980) "Cyclic Simple Shear Tests on Saturated Sand in Multi-Directional Loading", Soils and Foundations, Vol.20, No.1, 45-59.

Seed,H.B. and Idriss,I.M. (1970) "Soil Moduli and Damping Factors for Dynamic Response Analyses", EERC 70-10, Univ. California.

Tamura,C. and Suzuki,T. (1987) "A Quasi-Three-Dimensional Ground Model for Earthquake Response Analysis of Underground Structures - Construction of Ground Model -", Journal of Institute of Industrial Science, University of Tokyo.

Towhata,I. (1986) "Finite Element Model to Predict Permanent Displacement of Ground Induced by Liquefaction", Proc. 2nd Int. Conf. Numerical Models in Geomechanics, Ghent, 689-697.

Towhata,I. (1987) "Pseudo-Three-Dimensional Analysis of Dynamic Differential Motion of Liquefied Ground", Aseismic Design of Buried Pipelines with Special Consideration to Soil Liquefaction, ADEP Report, Tokyo, pp.93-115.

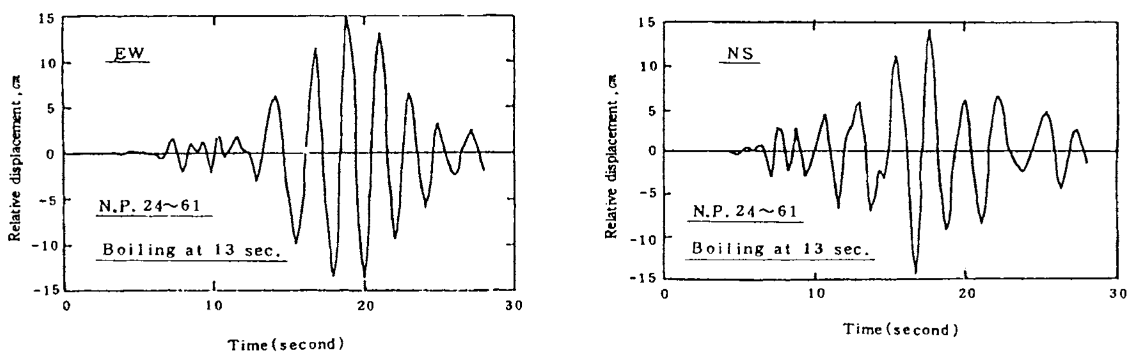

Fig.13 Effects of boiling on relative displacement of ground (Noshiro No.2).